



## Hollow Fiber Membrane Modules for NO<sub>x</sub> Removal using a Mixture of NaClO<sub>3</sub> and NaOH Solutions in the Shell Side as Absorbents

Eva F. Karamah<sup>1</sup>, Dwira S. Arbi<sup>1</sup>, Imanuel Bagas<sup>1</sup>, Sutrasno Kartohardjono<sup>1\*</sup>

<sup>1</sup>*Process Intensification Laboratory, Department of Chemical Engineering, Faculty of Engineering, Universitas Indonesia, Kampus UI Depok, Depok 16424, Indonesia*

**Abstract.** Nitrogen oxide (NO<sub>x</sub>) is one of the polluting gases harmful to humans and the environment. Nitrous oxide gas is mostly found in air, namely nitrogen monoxide (NO) and nitrogen dioxide (NO<sub>2</sub>). Nitrogen oxide gas in the air, which mostly comes from exhaust gases, needs to be reduced to minimize the threats to humans and the environment and comply with applicable regulations regarding hazards. The absorption process with a membrane contactor is an alternative to reduce NO<sub>x</sub> concentrations in the air. This study evaluates the hollow fiber membrane modules' performance in the NO<sub>x</sub> absorption process using sodium chlorate (NaClO<sub>3</sub>) and sodium hydroxide (NaOH) together as an absorbent solution. Based on the experimental results, the NO<sub>x</sub> reduction efficiency increased from 96.3 to 99.2% and from 99.4 to 99.7% with an increase in the concentration of NaClO<sub>3</sub> from 0.02 to 0.05 M and the number of fibers in the membrane module from 50 to 150. However, the absorption efficiency declined from 99.7 to 99.2% by increasing the feed gas flow rate from 100 to 200 mL/min. The highest value of NO<sub>x</sub> reduction efficiency, the overall mass transfer coefficient, the flux, and the NO<sub>x</sub> loading obtained in the study were 99.7%, 0.01743 cm s<sup>-1</sup>, 9.510×10<sup>-8</sup> mmole cm<sup>-2</sup> s<sup>-1</sup>, and 0.026 mole NO<sub>x</sub>/mole NaClO<sub>3</sub>, respectively.

**Keywords:** Absorption efficiency; Hollow fiber membrane module; NaClO<sub>3</sub>; NaOH; NO<sub>x</sub>

### 1. Introduction

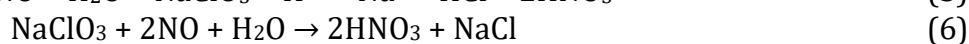
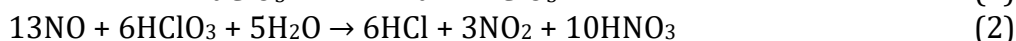
In the 21<sup>st</sup> century, air pollution has become one of the global community's problems of concern. Pollutants cause air pollution from harmful gases, one of which is nitrogen oxide (NO<sub>x</sub>) such as NO and NO<sub>2</sub>. Nitrogen oxide gas is generally formed from the combustion process with a high temperature above 300°C (Tan et al., 2019). Fifty-five percent of NO<sub>x</sub> gas comes from motor vehicles, and 45% comes from the industries' combustions process. High NO<sub>x</sub> levels in the atmosphere are the leading cause of acid rain, smog formation, decreased water quality, and global warming (Skalska et al., 2010; Gao et al., 2018; Sun et al., 2019; Mohan et al., 2020). Moreover, exposure to NO<sub>x</sub> gas with a 50-100 ppm concentration can cause lung inflammation from a health perspective. If the NO<sub>x</sub> concentration reaches 500 ppm, the people who inhale will inevitably die within 2-10 days (Shaw and Chadwick, 1998).

According to Government Regulation No. 45/1997, the quality standard for NO<sub>x</sub> in the air is 100µg/Nm<sup>3</sup> or about 0.05 ppm (Ministry of Environment RI, 1997). Various technologies have been developed to reduce the NO<sub>x</sub> concentration in the air.

\*Corresponding author's email: [sutrasno@che.ui.ac.id](mailto:sutrasno@che.ui.ac.id), Tel.: +62-21-7863516; Fax: +62-21-7863515  
doi: [10.14716/ijtech.v12i4.4408](https://doi.org/10.14716/ijtech.v12i4.4408)

These technological developments include dry methods, such as Selective Catalytic Reduction (SCR) and Selective Non-catalytic Reduction (Brandenberger et al., 2008) and wet methods, such as absorption using absorbents (Kartohardjono et al., 2019a; Fangyang et al., 2020). The SCR method uses  $\text{NH}_3$  as a reducing agent over catalysts based on  $\text{V}_2\text{O}_5\text{-WO}_3/\text{TiO}_2$  or Cu- and Fe-zeolite, which is very efficient to reduce  $\text{NO}_x$  but requires high temperatures around 300 to 400°C (Grossale et al., 2008; Mehring et al., 2012; Wang et al., 2019). The dry methods widely used are low- $\text{NO}_x$  burners and SCR, which have the disadvantages of low-efficiency and high investment costs, making the wet methods attractive to many researchers (Guo et al., 2018; Kartohardjono et al., 2019a). The wet methods through absorption in the conventional gas-liquid contactor still have disadvantages such as the relatively low contact surface area between 25-75  $\text{ft}^2/\text{ft}^3$ , thereby reducing the mass transfer. One alternative technology for  $\text{NO}_x$  gas absorption to increase the contact surface area is using a membrane module as a gas-liquid contactor (Cai et al., 2019).

Several previous studies have been conducted regarding  $\text{NO}_x$  absorption through a membrane contactor using a mixture of solutions functioning as an oxidizer and absorbent. The effective oxidizing agents include  $\text{NaClO}_3$ ,  $\text{NaClO}_2$ ,  $\text{KMnO}_4$ , and  $\text{H}_2\text{O}_2$  with the addition of  $\text{NaOH}$  or  $\text{HNO}_3$  as an absorbent (Yan et al., 2018; Kartohardjono et al., 2019a; Kartohardjono et al., 2020). Sodium chlorate and  $\text{NaClO}_2$  showed good  $\text{NO}_x$  absorption efficiency (> 90%) with the bubble column reactor media. A study by Shi et al. (2019) with  $\text{NaClO}_3/\text{NaOH}$  solvents conducted in the bubble column reactor media showed promising results with the highest  $\text{NO}_x$  absorption efficiency achieved, namely 91.5%. This study aims to see the polysulfone-based hollow fiber membrane modules' ability as media for the  $\text{NO}_x$  gas absorption process using a mixture of  $\text{NaClO}_3$  and  $\text{NaOH}$  solutions as an absorber. The reaction mechanism of  $\text{NO}_x$  absorption by  $\text{NaClO}_3$  may occur as follows (Shi et al., 2019):



This study also aims to see the effect of  $\text{NaClO}_3$  concentration, the number of fibers in the membrane module, and  $\text{NO}_x$  gas flow rate on the  $\text{NO}_x$  absorption performance, such as  $\text{NO}_x$  absorption efficiency ( $R$ ), mass transfer coefficient ( $K_G$ ), mass transfer flux ( $J$ ), and  $\text{NO}_x$  loading.

## 2. Methods

Figure 1 shows a schematic diagram of the experimental set-up for removing  $\text{NO}_x$  from the gas stream through a hollow fiber membrane module. The membrane modules used—purchased from GDP Filter Bandung, Indonesia—contain 50, 100, and 150 polysulfone-based fibers with an internal and external diameter of 0.18 mm and 0.20 mm, respectively, and a length of 25 cm, giving an effective surface area of approximately 0.0785, 0.157, and 0.2355  $\text{m}^2$ , respectively. The  $\text{NaClO}_3$  and  $\text{NaOH}$  used are supplied by Merck, Indonesia, while the gas feed—which contains  $\text{NO}_x$  of around 560 ppm in nitrogen ( $\text{N}_2$ )—is purchased from Energi Indogas Nusantara. During the experiment, the feed gas entered the membrane module through the lumen fibers, and the flow rate was adjusted using the CX series mass flow controller, Shanghai Instrument, while the composition was measured using the Gas Analyzer, Ecom-D. The feed gas is then diffused through fiber pores into the shell side of the

membrane module containing absorbent solutions. The feed gas flow rate applied in the experiment were 100, 125, 150, 175, and 200 mL/minute, and the variation in the concentration of NaClO<sub>3</sub> was 0.01, 0.02, 0.03, 0.04, and 0.05 M, respectively.

The  $R$  of NO<sub>x</sub> is one of the parameters to determine the amount of NO<sub>x</sub> gas absorbed by the absorbent in the hollow fiber membrane module. This parameter shows the ratio between the amount of NO<sub>x</sub> gas absorbed by the solvent and the amount of NO<sub>x</sub> gas in the feed. The higher the absorption efficiency indicates, the better the NO<sub>x</sub> absorption process. Other parameters observed in the experiment are the overall mass transfer coefficient,  $K_G$ , flux,  $J$ , and NO<sub>x</sub> loading, which are all calculated by (Wang et al., 2004; Wang and Yu, 2017; Kartohardjono et al., 2019):

$$R = \frac{C_{NO_{x\text{in}}} - C_{NO_{x\text{out}}}}{C_{NO_{x\text{in}}}} \quad (7)$$

$$K_G = \frac{Q_G}{A_m} \ln \left( \frac{C_{NO_{x\text{in}}}}{C_{NO_{x\text{out}}}} \right) \quad (8)$$

$$J = \frac{(C_{NO_{x\text{in}}} - C_{NO_{x\text{out}}})}{A_m} Q_G \frac{P}{RT} \quad (9)$$

$$NO_{x\text{-loading}} = \frac{\text{mole } NO_{x\text{-abs}}}{\text{mole } NaClO_3} \quad (10)$$

$$\text{mole } NO_{x\text{-abs}} = (C_{NO_{x\text{in}}} - C_{NO_{x\text{out}}}) Q_G \frac{P}{RT} \quad (11)$$

where  $C_{NO_{x\text{in}}}$ ,  $C_{NO_{x\text{out}}}$ ,  $Q_G$ , and  $A_m$  are the concentration of NO<sub>x</sub> inlet and outlet of the membrane module, the feed gas flow rate, and the membrane surface area, respectively. Meanwhile,  $P$ ,  $T$ , and  $R$  are atmospheric pressure, temperature, and ideal gas constant, respectively.

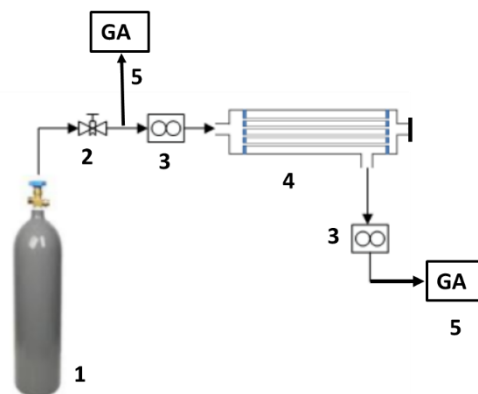


**Figure 1** Experiment set-up and apparatus: 1. Feed gas containing NO<sub>x</sub> of around 560 ppm; 2. Valve; 3. Mass flow controller; 4. Hollow fiber membrane module; 5. Gas analyzer

### 3. Results and Discussion

#### 3.1. Effects of Feed Gas Flow Rate

Figure 2 shows the dependence of the NO<sub>x</sub> reduction efficiency on feed gas flow and the amount of fibers in the membrane module. As shown in Figure 2, the NO<sub>x</sub> absorption efficiency declines with an increase in the feed gas flow rate. The process of gas transfer to the gas-liquid membrane contactor occurs in three stages: (a) the gas is transferred to the inner surface of the fibers; (b) the gas diffuses through the pores of the fibers; and (c) the gas is absorbed in the shell side of membrane module by absorbent, where the reaction occurred as shown in Equations (1-6) (Wang and Yu, 2017; Kartohardjono et al., 2019a; Kartohardjono et al., 2019b). Of the three stages of the mass transfer process, one of the influencing factors

is the gas's residence time in the membrane fibers. The longer the gas's residence time in the membrane module, the better the transfer process is due to the longer contact time between the gas and the membrane surface.

The experimental results indicated that an increase in the NO<sub>x</sub> gas flow rate reduced NO<sub>x</sub> absorption efficiency. The NO<sub>x</sub> reduction efficiency decreases when increasing the flow rate of feed gas due to the lower residence time of the gas in the membrane fibers, which reduces the time for gas-absorbent contact so that less NO<sub>x</sub> gas is absorbed (Kartohardjono et al., 2019a; Kartohardjono et al., 2020). The efficiency of NO<sub>x</sub> absorption in the study decreased from 99.6 to 98.9% if the feed gas flow rate was increased from 0.1 to 0.2 L/min in the membrane module containing 100 fibers and 150 ml solutions of 0.05 M NaClO<sub>3</sub> and NaOH, respectively. Previous studies also showed a similar trend where NO<sub>x</sub>'s absorption efficiency decreased from 98 to 94% using the same membrane module containing 150 ml of 0.25 wt.% H<sub>2</sub>O<sub>2</sub> and 0.25 M HNO<sub>3</sub> solution as absorbent (Kartohardjono et al., 2019a). Meanwhile, another study reported that NO<sub>x</sub> removal efficiency declined from about 91 to 29% when the flow rate of feed gas increased from 0.05 to 0.25 L/min in a hollow fiber membrane module of polypropylene-based using the NO<sub>x</sub> concentration in the feed gas of about 184.8 ppm, and when the absorbent solution contains a mixture of 5 wt.% NaCl and 0.2 wt.% H<sub>2</sub>O<sub>2</sub> (Wang and Yu, 2017). Figure 2 also demonstrated that the efficiency of NO<sub>x</sub> absorption enhances with the increasing amount of fibers due to the rise in the gas-liquid phases' contact area in the hollow fiber membrane, thereby increasing NO<sub>x</sub> gas absorbed and leading to an increase in the NO<sub>x</sub> absorption efficiency (Kartohardjono et al., 2020).

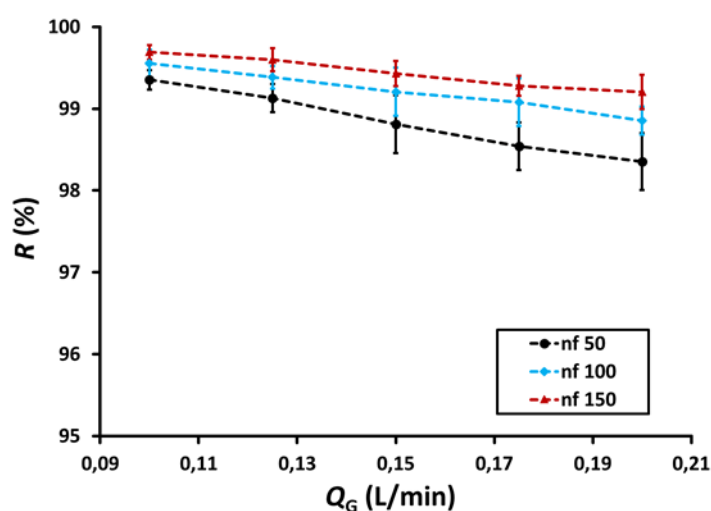


**Figure 2** The influences of the flow rate of the feed gas,  $Q_G$ , on the NO<sub>x</sub> removal efficiency,  $R$ , at various numbers of fibers in the membrane modules,  $n_f$ , containing 150 mL of 0.05 M NaClO<sub>3</sub> and NaOH solutions

Figure 3 shows the overall mass transfer coefficient and flux dependence on feed gas flow and the number of fibers in the membrane module. The overall mass transfer coefficient and flux, as shown in Figure 3, increases with an increase in the flow rate of feed gas due to decreasing the gas-liquid boundary layer's thickness, thereby decreasing the mass transfer resistance. Figure 3 also demonstrates that the overall mass transfer coefficient and flux decline with the increasing amount of membrane fibers used. Increasing the amount of fibers in the membrane increases the surface area for gas-liquid contact, thereby increasing the amount of NO<sub>x</sub> absorbed. However, increasing the membrane's

surface area can also reduce the overall mass transfer coefficient and flux, as in Equations 8 and 9. The decrease in the overall mass transfer coefficient and flux on the increase in the number of fibers indicates that the surface area effect is more dominant than the amount of NO<sub>x</sub> absorbed (Kartohardjono et al., 2019a). Figure 3 also shows that an increase in the feed gas flow rate also increases the overall mass transfer coefficient and flux due to the decrease in the boundary layer thickness in the gas phase, which increases the overall mass transfer coefficient and flux. The amount of NO<sub>x</sub> present in the feed gas increases with the feed gas flow rate, thereby increasing the NO<sub>x</sub> transfer's driving force, which leads to increasing the overall mass transfer coefficient and flux. The thickness of the gas-liquid boundary layer decreases as the feed gas flow rate increases, enhancing the gas diffusion process (Kartohardjono et al., 2020). Similar results were also presented by Fangyang et al. (2020), where the flux of NO<sub>x</sub> increased from about 7.0 to 16.5 mole m<sup>-2</sup> h<sup>-1</sup> when the feed gas flow rate increased from about 60 to 200 cm<sup>3</sup> min<sup>-1</sup>, in the ceramic membrane module using absorbent of 5 wt.% NaCl and 0.2 wt.% H<sub>2</sub>O<sub>2</sub>, the flow rate of absorbent of 40 cm<sup>3</sup> min<sup>-1</sup>, and temperature of absorbent of 343 K. The overall mass transfer coefficient and flux, as presented in Figure 2, declines with increasing the number of fibers in the membrane module due to the increment in the gas-liquid contact area (Kartohardjono et al., 2019a).

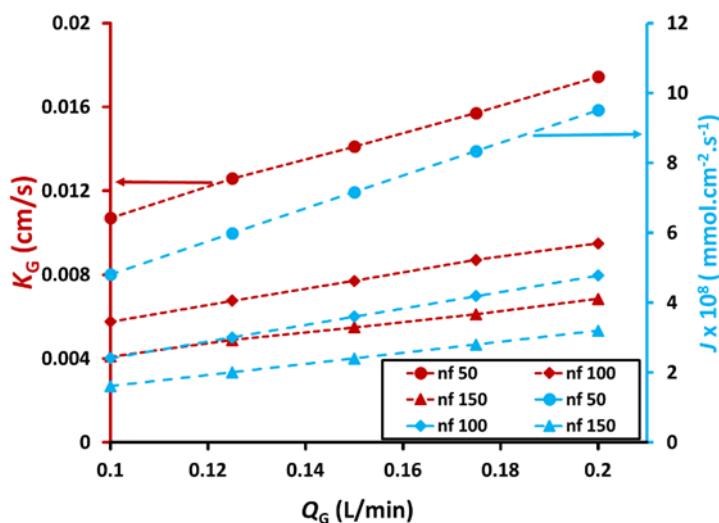
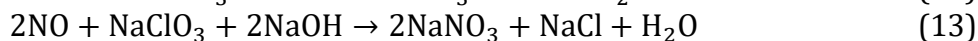
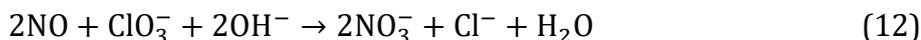


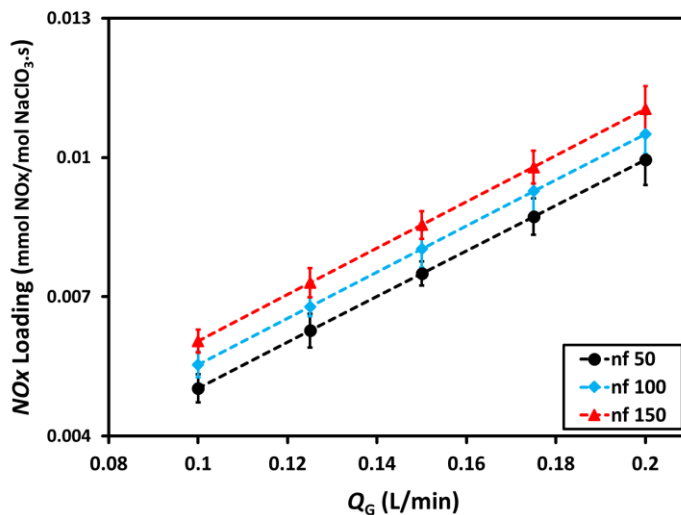
**Figure 3** The influences of the feed gas flow rate,  $Q_G$ , on the overall mass transfer coefficient,  $K_G$ , and flux,  $J$ , on the various amount of fibers in the membrane modules,  $n_f$ , containing 150 mL of 0.05 M NaClO<sub>3</sub> and NaOH solutions

The dependence of NO<sub>x</sub> loading on the flow rate of the feed gas is demonstrated in Figure 4. This parameter is determined by calculating the ratio of moles of NO<sub>x</sub> absorbed and the moles of absorbent used. The absorbent used in the study was a mixture of NaClO<sub>3</sub> and NaOH solutions. The number of moles of solvent used in the calculation is only NaClO<sub>3</sub> species due to its role as an oxidizing agent for NO<sub>x</sub> gas based on the reaction (Shi et al., 2019):



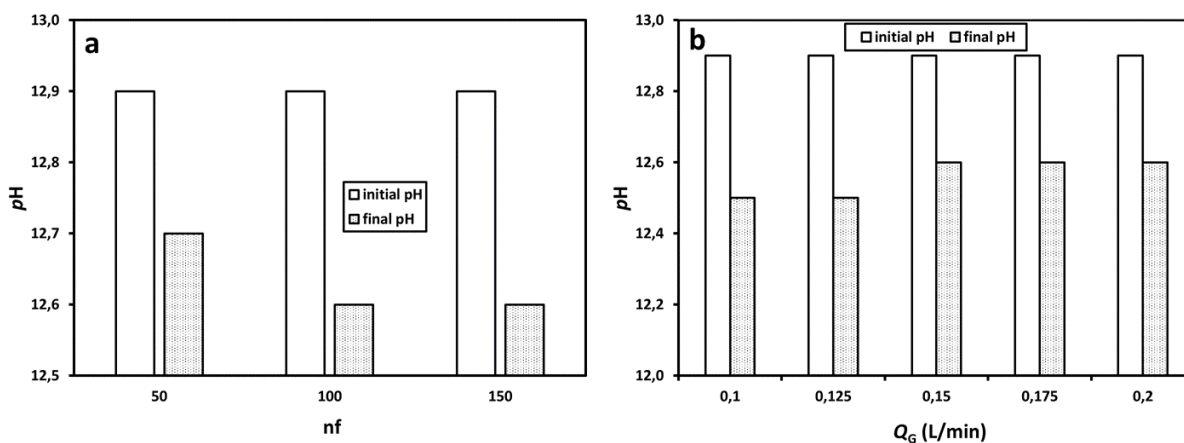
As shown in Figure 4, the NO<sub>x</sub> loading increases when the feed gas's flow rate increases due to an increase in the concentration gradient in the gas-liquid phases and a decrease in the boundary layer's thickness, which enhances the mass transfer process (Kartohardjono et al., 2019a). The mass transfer enhancement increases the amount of NO<sub>x</sub> absorbed by the absorbents and finally increases the NO<sub>x</sub> loading. The NO<sub>x</sub> loading also increases with

the number of fibers used due to an increase in the gas-liquid contact area. The higher the gas-liquid contact area, the more NOx can be absorbed by the solvent, which leads to an increase in NOx loading (Kartohardjono et al., 2017).



**Figure 4** The influences of the feed gas flow rate,  $Q_G$ , on the NOx loading at various membrane modules,  $n_f$ , containing 150 mL of 0.05 M NaClO<sub>3</sub> and NaOH solutions

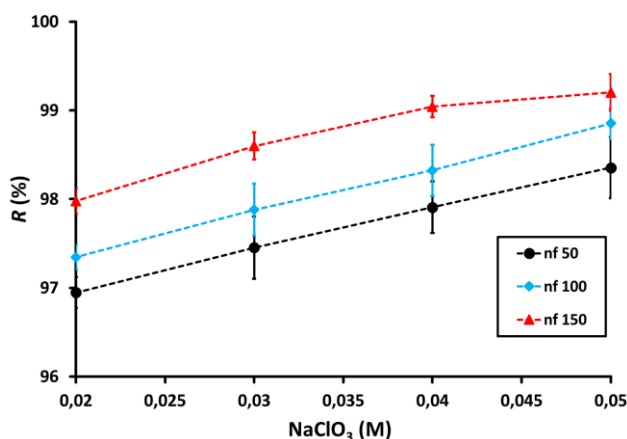
The change in the absorbents' pH for one hour of the absorption process is shown in Figure 5. The reaction occurred between NOx and NaClO<sub>3</sub> and NaOH during the absorption process to produce NO<sub>3</sub><sup>-</sup> and Cl<sup>-</sup> as presented in Equations (12 and 13), causing a decreased pH, as demonstrated in Figure 5. Figure 5a shows that, as the number of fibers increases, the final measured pH decreases due to more NOx being absorbed. As a result, more NOx in the feed gas reacts with the absorbents to increase NaNO<sub>3</sub> and NaCl products, which increases the pH drop. Figure 5b, on the other hand, shows that the higher the flow rate of the feed gas, the lower the decrease in absorbent pH due to less NOx being absorbed.



**Figure 5** (a) The pH of absorbents before and after the absorption process at the feed gas flow rate,  $Q_G$ , of 0.2 L/min at the various amount of fibers in the membrane modules containing 150 mL of 0.05 M NaClO<sub>3</sub> and NaOH solutions; (b) The pH of absorbents before and after the absorption process in the membrane module consists of 150 fibers containing 150 mL of 0.05 M NaClO<sub>3</sub> and NaOH solutions at various feed gas flow rates,  $Q_G$

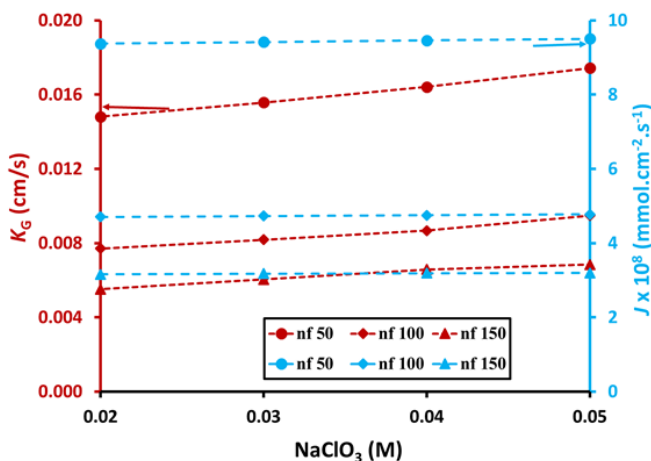
### 3.2. Effects of Absorbent Concentration

Figure 6 shows that increasing the concentration of NaClO<sub>3</sub> in the absorbent solution causes an increase in NO<sub>x</sub> absorption efficiency. Sodium chlorate dissociates into ClO<sub>3</sub><sup>-</sup> ions in water and NaOH solutions, where ClO<sub>3</sub><sup>-</sup> then oxidizes NO to NO<sub>2</sub> and then re-oxidizes it to NaNO<sub>3</sub>. As shown in Equations 12 and 13, the reactions depend on the number of moles of NaClO<sub>3</sub>, which is thermodynamically spontaneous and irreversible (Guo et al., 2010). Increasing the concentration of NaClO<sub>3</sub> is directly proportional to the number of moles of NaClO<sub>3</sub> in the solution so that the NO<sub>x</sub> absorption rate increases with the increasing concentration of NaClO<sub>3</sub>. The study's results follow previous studies stating that increasing the concentration of NaClO<sub>3</sub> can increase the absorption rate of NO<sub>x</sub> (Guo et al., 2010). Another similar study conducted by Shi et al. (2019) using a bubble column reactor also showed similar results where an increase in the concentration of NaClO<sub>3</sub> from 0.005 M to 0.1 M led to an increase in NO<sub>x</sub> absorption efficiency from 35.48 to 91.65%. As presented in Figure 6, the increment of fibers also increases NO<sub>x</sub> absorption efficiency due to more contact surface area for gas-liquid phases in the membrane module. The highest NO<sub>x</sub> absorption efficiency obtained from this study was 99.2% at a flow rate of 200 mL/min containing NO<sub>x</sub> of about 560 ppm, the number of fibers in the membrane module of 150 containing 0.05M NaClO<sub>3</sub> and NaOH in the 150 mL of absorbent solution. This result was better than the study conducted by Shi et al. (2019), in a bubble column reactor, obtained the highest NO<sub>x</sub> absorption efficiency of 91.65% using 500 mL of 0.1 M NaClO<sub>3</sub> as absorbents, and the flow rate of a feed gas of 160 mL/min having NO<sub>x</sub> of about 800 ppm.



**Figure 6** The effects of the NaClO<sub>3</sub> concentration in absorbent solutions on the NO<sub>x</sub> removal efficiency,  $R$ , at various membrane modules,  $n_f$ , containing 150 mL of absorbent solutions and the feed gas flow rate of 0.2 L/minute

The overall mass transfer coefficient and flux, as shown in Figure 7, were slightly enhanced with an increase in the NaClO<sub>3</sub> concentration in the absorbent solution. The overall mass transfer coefficient and flux only slightly increase with increasing NaClO<sub>3</sub> concentration. The main driving force in the NO<sub>x</sub> removal process in the membrane module is the NO<sub>x</sub> concentration difference in the gas and liquid phases (Kartohardjono et al., 2019a). Increasing the concentration of NaClO<sub>3</sub> in the absorbent solution only slightly increases the reaction rate between NO<sub>x</sub> and NaClO<sub>3</sub> as almost all of the NO<sub>x</sub> in the feed gas has been absorbed, indicated by the absorption efficiency, which was above 90%. Therefore, it only causes a slight increase in the overall mass transfer coefficient and flux.



**Figure 7** The effects of the NaClO<sub>3</sub> concentration in absorbent solutions on the overall mass transfer coefficient,  $K_G$ , and flux,  $J$ , at the various membrane modules,  $n_f$ , containing 150 mL of absorbent solutions and the feed gas flow rate of 0.2 L/minute

Figure 8 illustrates the influence of NaClO<sub>3</sub> concentration in the absorbent solution on the NO<sub>x</sub> loading at the feed gas flow rate of 0.2 L/min. Nitrogen oxide loading decreases with increasing NaClO<sub>3</sub> concentration due to the increase in the amount of NO<sub>x</sub> absorbed not being proportional to the increase in NaClO<sub>3</sub> concentration in the absorbent solution. Meanwhile, as predicted, NO<sub>x</sub> loading increases with increasing fibers due to more contact area in the gas-liquid phases. The highest NO<sub>x</sub> loading obtained was 0.026 mole NO<sub>x</sub>/mole NaClO<sub>3</sub> in a 150 fibers membrane module containing 0.01 M NaClO<sub>3</sub> in absorbent solution and a flow rate of a feed gas of 0.2 L/ minute.

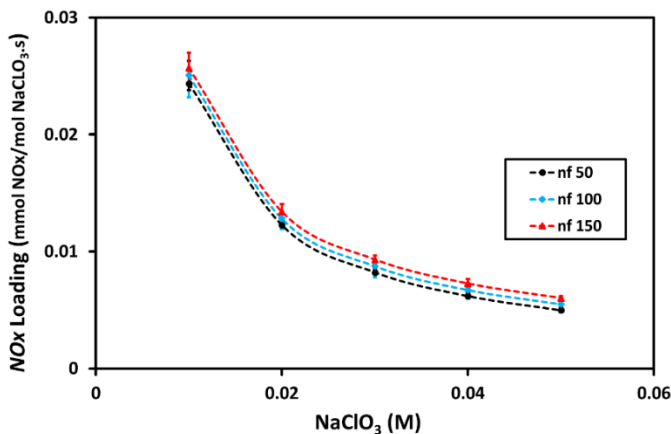


**Figure 8** The variation of NO<sub>x</sub> loading with the concentration of NaClO<sub>3</sub> in absorbent solutions on the NO<sub>x</sub> loading at the various membrane modules,  $n_f$ , containing 150 mL of absorbent solutions and the feed gas flow rate of 0.2 L/minute

#### 4. Conclusions

The study has been conducted to reduce the NO<sub>x</sub> concentration from its mixture with N<sub>2</sub> in the hollow fiber membrane modules using an absorbent of a mixture of NaClO<sub>3</sub> and NaOH solutions. The experimental results confirmed that the gas stream's NO<sub>x</sub> concentration could be drastically reduced through the proposed process. The NO<sub>x</sub>'s absorption efficiency increased with increasing NaClO<sub>3</sub> concentration in the absorbent solution and the amount of fibers in the membrane module. However, the NO<sub>x</sub>'s absorption

efficiency declined as the feed gas flow rate increased. The best results from experiments on the NO<sub>x</sub> absorption efficiency, the overall mass transfer coefficient, the flux, and the NO<sub>x</sub> loading were 99.7%, 0.01743 cm s<sup>-1</sup>, 9.510×10<sup>-8</sup> mmole cm<sup>-2</sup> s<sup>-1</sup>, and 0.026 mole NO<sub>x</sub>/mole NaClO<sub>3</sub>, respectively.

### Acknowledgements

The authors wish to acknowledge the financial support for this study from the PDUPT Project via the Directorate of Research and Services Universitas Indonesia through Contract No. NKB-267/UN2.RST/HKP.05.00/2020.

### References

- Brandenberger, S., Kröcher, O., Tissler, A., Althoff, R., 2008. The State of the Art in Selective Catalytic Reduction of NO<sub>x</sub> by Ammonia using Metal-exchanged Zeolite Catalysts. *Catalysis Reviews - Science and Engineering*, Volume 50(4), pp. 492–531
- Cai, Y., Luo, Y., Chu, G.-W., Wu, W., Yu, X., Sun, B.-C., Chen, J.-F., 2019. NO<sub>x</sub> Removal in a Rotating Packed Bed: Oxidation and Enhanced Absorption Process Optimization. *Separation and Purification Technology*, Volume 227, doi.org/10.1016/j.seppur.2019.115682
- Fangyang, Y., Jiali, Y., Wei, Y., Jiyun, D., Jianfeng, Y., 2020. Nitric Oxide Reduction by Hydrogen Peroxide Absorption through a Ceramic Hollow Fiber Membrane Contactor. *Journal of Environmental Chemical Engineering*, Volume 8(5), p. 104129
- Gao, L., Li, C., Lu, P., Zhang, J., Du, X., Li, S., Tang, L., Chen, J., Zeng, G., 2018. Simultaneous Removal of Hg<sub>0</sub> and NO from Simulated Flue Gas Over Columnar Activated Coke Granules Loaded with La<sub>2</sub>O<sub>3</sub>-CeO<sub>2</sub> at Low Temperature. *Fuel*, Volume 215, pp. 30–39
- Grossale, A., Nova, I., Tronconi, E., 2008. Study of a Fe-zeolite-based System as NH<sub>3</sub>-SCR Catalyst for Diesel Exhaust Aftertreatment. *Catalysis Today*, Volume 136(1-2), pp. 18–27
- Guo, R.-t., Gao, X., Pan, W.-g., Ren, J.-x., Wu, J., Zhang, X.-b., 2010. Absorption of NO into NaClO<sub>3</sub>/NaOH Solutions in a Stirred Tank Reactor. *Fuel*, Volume 89(11), pp. 3431–3435
- Guo, L., Han, C., Zhang, S., Zhong, Q., Ding, J., Zhang, B., Zeng, Y., 2018. Enhancement Effects of O<sub>2</sub><sup>-</sup> and OH Radicals on NO<sub>x</sub> Removal in the Presence of SO<sub>2</sub> by using an O<sub>3</sub>/H<sub>2</sub>O<sub>2</sub> AOP System with Inadequate O<sub>3</sub> (O<sub>3</sub>/NO molar ratio= 0.5). *Fuel*, Volume 233, pp. 769–777
- Kartohardjono, S., Merry, C., Rizky, M.S., Pratita, C.C., 2019a. Nitrogen Oxide Reduction through Absorbent Solutions Containing Nitric Acid and Hydrogen Peroxide in Hollow Fiber Membrane Modules. *Heliyon*, Volume 5(12), doi.org/10.1016/j.heliyon.2019.e02987
- Kartohardjono, S., Saksono, N., Supramono, D., Prawati, P., 2019b. NO<sub>x</sub> Removal from Air through Super Hydrophobic Hollow Fiber Membrane Contactors. *International Journal of Technology*, Volume 10(3), pp. 472–480
- Kartohardjono, S., Paramitha, A., Putri, A.A., Andriant, R., 2017. Effects of Absorbent Flow Rate on CO<sub>2</sub> Absorption through a Super Hydrophobic Hollow Fiber Membrane Contactor. *International Journal of Technology*, Volume 8(8), pp. 1429–1435
- Kartohardjono, S., Rizky, M.S., Karamah, E.F., Lau, W.J., 2020. The Effect of the Number of fibers in Hollow Fiber Membrane Modules for NO<sub>x</sub> Absorption. *International Journal of Technology*, Volume 11(2), pp. 269–277
- Mehring, M., Elsener, M., Kröcher, O., 2012. Selective Catalytic Reduction of NO<sub>x</sub> with Ammonia Over Soot. *ACS Catalysis*, Volume 2(7), pp. 1507–1518

- Ministry of Environment RI*, 1997. Decree of The State Minister of the Minister of the Environment, No. Kep-45/MenLH/10/1997, Concerning Air Pollution Standard Index. Jakarta
- Mohan, S., Dinesha, P., Kumar, S., 2020. NO<sub>x</sub> Reduction Behaviour in Copper Zeolite Catalysts for Ammonia SCR systems: A Review. *Chemical Engineering Journal*, Volume 384(31), doi.org/10.1016/j.cej.2019.123253
- Shaw, I., Chadwick, J., 1998. Principles of Environmental Toxicology. CRC Press, USA
- Shi, D., Sun, G., Cui, Y., 2019. Study on the Removal of NO from Flue Gas by Wet Scrubbing using NaClO<sub>3</sub>. *Journal of the Serbian Chemical Society*, Volume 84(10), pp. 53–53
- Skalska, K., Miller, J.S., Ledakowicz, S., 2010. Trends in NO<sub>x</sub> abatement: A Review. *Science of the Total Environment*, Volume 408(19), pp. 3976–3989
- Sun, P., Cheng, X., Wang, Z., Lai, Y., Ma, C., Chang, J., 2019. NO<sub>x</sub> Reduction by CO Over ASC Catalysts in a Simulated Rotary Reactor: Effect of Reaction Conditions. *Journal of the Energy Institute*, Volume 92(3), pp. 488–501
- Tan, L., Guo, Y., Liu, Z., Feng, P., Li, Z., 2019. An Investigation on the Catalytic Characteristic of NO<sub>x</sub> Reduction in SCR Systems. *Journal of the Taiwan Institute of Chemical Engineers*, Volume 99, pp. 53–59
- Wang, D., Teo, W., Li, K., 2004. Selective Removal of Trace H<sub>2</sub>S from Gas Streams Containing CO<sub>2</sub> using Hollow Fibre Membrane Modules/Contractors. *Separation and Purification Technology*, Volume 35(2), pp. 125–131
- Wang, Y., Yu, X., 2017. Removal of NO Research in A Polypropylene Hollow Fiber Membrane Contactor. In: The 2017 6<sup>th</sup> International Conference on Energy, Environment and Sustainable Development (ICSD 2017)
- Wang, Z.-y., Guo, R.-t., Shi, X., Pan, W.-g., Liu, J., Sun, X., Liu, S.-w., Liu, X.-y., Qin, H., 2019. The Enhanced Performance of Sb-modified Cu/TiO<sub>2</sub> Catalyst for Selective Catalytic Reduction of NO<sub>x</sub> with NH<sub>3</sub>. *Applied Surface Science*, Volume 475, pp. 334–341
- Yan, Q., Chen, S., Zhang, C., O'Hare, D., Wang, Q., 2018. Synthesis of Cu<sub>0.5</sub>Mg<sub>1.5</sub>Mn<sub>0.5</sub>Al<sub>0.5</sub>O<sub>x</sub> Mixed Oxide from Layered Double Hydroxide Precursor as Highly Efficient Catalyst for Low-Temperature Selective Catalytic Reduction of NO<sub>x</sub> with NH<sub>3</sub>. *Journal of Colloid and Interface Science*, Volume 526, pp. 63–74